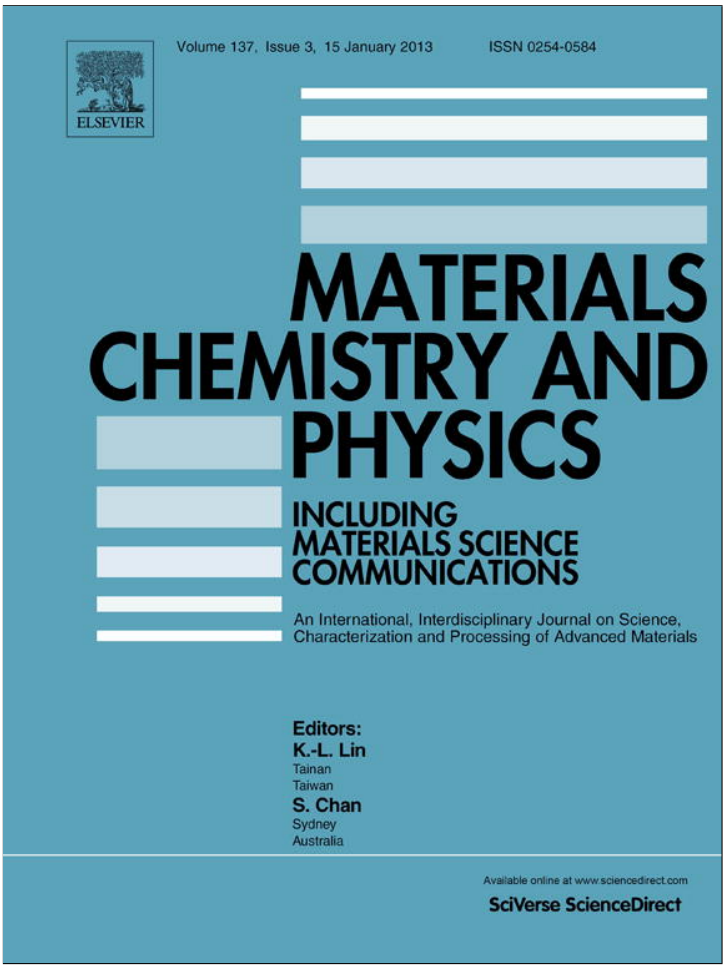

Materials Chemistry and Physics 137 (2013) 1007–1011

Contents lists available at SciVerse ScienceDirect

Materials Chemistry and Physics

journal homepage: www.elsevier.com/locate/matchemphys

Size-dependent melting point of nanoparticles based on bond number calculation

H. Li [a], P.D. Han [a], X.B. Zhang [b], M. Li [b,*]

[a] College of Materials Science and Engineering, Taiyuan University of Technology, Taiyuan 030024, China
[b] School of Physics and Electric Information, Huaibei Normal University, Huaibei 235000, China

HIGHLIGHTS

- An united model for melting point or cohesive energy of nanoparticles is established.
- Decreased cohesive energy or melting point arises from the lowered bond number.
- Good estimation of the model is obtained even nanoparticle's structure is unknown.

ARTICLE INFO

Article history:
Received 12 October 2011
Received in revised form
16 October 2012
Accepted 7 November 2012

Keywords:
Metals
Nanostructures
Crystal structure
Thermodynamic properties

ABSTRACT

An integrated model based on bond number and bond strength in a system with a cubo-octahedral structure is developed to predict the size-dependent thermal characteristics of nanoparticles. Without any adjustable parameters, this model can be used to predict the melting point and cohesive energy of low-dimensional materials, suggesting that both depend on the size and on the atomic distance. The good agreement of the theoretical prediction with the experimental and molecular dynamic simulation results confirms the validity of the cubo-octahedron in describing the thermodynamic behaviors of nanoparticles even without considering their crystalline structures.

1. Introduction

The thermodynamic behavior of nanocrystals differs from that of their corresponding bulk materials mainly because of the large surface-to-volume ratio that strongly influences the chemical [1] and physical properties of the nanocrystals [2,3]. The broken bonds of surface atoms inevitably lead to the instability of materials at the nanoscale (e.g., decreased melting point and cohesive energy of ultrafine metallic particles with decreased size). Thus, a number of excellent models for size and shape dependence of the melting behavior of a nanosolid have been developed in terms of classical thermodynamics and modern molecular dynamics [4–26]. In these models, the most important consideration is the surface-to-volume ratio because the vibration frequency of surface atoms is distinct from that of the inner ones. An exponential or linear relationship between the material size and thermodynamic function has been obtained, and the good reasonability of the established models has been proven. However, the bond characteristics of a system are unclear. In fact, the bond state of a system is directly related to the thermal properties. The atomic cohesive energy can be obtained from the average coordination number and bond strength per atom. In other words, if the bond number and bond strength are known, the thermodynamic function can be easily determined. Thus, the cohesive energy $E(D)$, where D is the nanocrystal size, can be expressed as follows [26]:

$$E(D) = B_a E_i(D) \quad (1)$$

where B_a and $E_i(D)$ are the bond number and average bond strength of a nanocrystal, respectively. Considering the broken bonds in nanocrystals, B_a decreases with decreased size, which inevitably results in decreased $E(D)$ function based on Eq. (1). Notably, the broken bonds in a system rely on surface structure (e.g., the number of broken bonds in the (111), (110), and (100) faces of the fcc crystal are 3, 4, and 6, respectively) [27]. This result indicates that B_a is related to size D and depends on the nanocrystal structure. Similarly, the $E(D)$ function can be easily considered.

The cohesive energy that directly describes the bond strength is an effective variable for determining the thermal stability of nanocrystals. With size reduction, the decline in the melting point

* Corresponding author.
E-mail address: liming2010@chnu.edu.cn (M. Li).

0254-0584/$ – see front matter © 2012 Elsevier B.V. All rights reserved.
http://dx.doi.org/10.1016/j.matchemphys.2012.11.016

$T_m(D)$ is an obvious phenomenon that describes the lowered thermal stability of nanocrystals. In fact, an empirical correlativity exists between the E_0 and T_{m0} functions by defining E_0 and T_{m0} as the bulk cohesive energy and bulk melting point, respectively [28]:

$$T_{m0} = 0.032E_0/k_B \tag{2.1}$$

where k_B is the Boltzmann constant. E_0 can be written as $E_0 = B_tE_{i0}$ based on Eq. (1), where B_t and E_{i0} are the total bond number without broken bonds and the average single bond energy for bulk crystal, respectively. According to Eq. (2.1), a similar treatment for the relationship between the $E(D)$ and $T_m(D)$ functions can be expected as a first approximation; thus,

$$T_m(D) = 0.032E(D)/k_B \tag{2.2}$$

Therefore, combining Eqs. (1) and (2) with the expression for the aforementioned above E_0 function yields,

$$T_m(D)/T_{m0} = E(D)/E_0 = B_aE_i(D)/B_tE_{i0} \tag{3}$$

Hence, four variables must be definitely known to obtain the $T_m(D)$ value. Generally, without considering bond relaxation, $E_i(D) \approx E_{i0}$ can be assumed for simplicity. Considering this approximation, Sanjabi et al. [29] and Vahdati-Khaki et al. [30] respectively developed the $E(D)/E_0$ and $T_m(D)/T_{m0}$ models by introducing the mean coordination number concept ($\overline{Z}_p/Z_b$, where $\overline{Z}_p$ and Z_b show the mean coordination number of a nanocrystal and its corresponding bulk, respectively); thus,

$$E(D)/E_0 = T_m(D)/T_{m0} = \overline{Z}_p/Z_b \tag{4}$$

The value of $\overline{Z}_p/Z_b$ in Eq. (4) is equal to that of B_a/B_t in Eq. (3). The validity of Eq. (4) has been confirmed by both Sanjabi et al. [29] and Vahdati-Khaki et al. [30], particularly when compared with metallic nanoparticles with $D > 10$ nm (where $E_i(D) \approx E_{i0}$ and a small difference can be widely accepted). However, neglecting bond relaxation inevitably leads to errors in the $E(D)$ function, especially for nanoparticles with $D < 10$ nm. Thus, the effect of bond relaxation on cohesive energy needs to be determined to establish a reasonable model for the $T_m(D)/T_{m0}$ or $E(D)/E_0$ function.

In this work, B_a/B_t is determined by introducing a cubo-octahedral structure and by considering reasonable bond relaxation. Models for $T_m(D)/T_{m0}$ and $E(D)/E_0$ are also developed. The model predictions are found to be consistent with experimental and simulation results for metallic nanoparticles. The validity of the model is also confirmed within the full size range.

2. Model

To determine the effect of surface relaxation on $E(D)$, which is neglected in Eq. (4), $E(D)$ is considered as an energetic sum of the surface and interior atoms. Thus, $E(D) = \delta(E_0 + \gamma) + (1 - \delta)E_0$ or:

$$E(D)/E_0 = 1 + \gamma\delta/E_0 \tag{5}$$

where δ is surface/volume ratio. The surface energy γ in Eq. (5) can be calculated by relating the bond deficit with the surface bond relaxation, which has been previously modeled [31]. Thus,

$$\gamma/E_0 = -\left[1 - (Z_s/Z_b)^{1/2}\right]. \tag{6}$$

where Z_s is the mean coordination number of the surface atoms of a cluster.

With the two boundary conditions of $\delta \ll 1$ with $Z_s \approx Z_{sb}$ (where Z_{sb} denotes the surface atom coordination number of bulk), and $\delta \to 1$, inserting Eq. (6) into Eq. (5) yields the two limit cases for $E(D)/E_0$:

$$E(D)/E_0 \approx 1 - \left[1 - (Z_{sb}/Z_b)^{1/2}\right]\delta \tag{7.1}$$

$$E(D)/E_0 \approx (Z_s/Z_b)^{1/2} \tag{7.2}$$

Letting N_s and N_i be the number of surface atoms and inner atoms, respectively, the common relationship is $B_a/B_t = (N_sZ_s + N_iZ_b)/(NZ_b)$, where $N_i = N - N_s$ and $N_s/N = d$. Thus,

$$B_a/B_t = 1 - \delta(1 - Z_s/Z_b) \tag{8}$$

From Eq. (8), $B_a/B_t \approx Z_s/Z_b$ when $\delta \to 1$. When $\delta \to 0$, $B_a/B_t \to (B_a/B_t)^{1/2} \to 1$. Substituting these results into Eq. (6) enables $E(D)$ to be rewritten as,

$$E(D)/E_b \approx (B_a/B_t)^{1/2} \tag{9}$$

Clearly, Eq. (8) applies to both limit cases of Eqs. (5) and (6) and is even confirmed applicable to any D [31]. However, the effect of surface relaxation on $E_i(D)$ in the deduction of Eq. (9) is overestimated because only attractive forces are taken into account [31], whereas it is underestimated in Eq. (4). To compensate for the deficiency in Eqs. (4) and (9), as a first approximation, a rough estimate of $E(D)$ values can be easily determined by considering the average effect of Eqs. (4) and (9):

$$E(D)/E_0 = \left[(B_a/B_t)^{1/2} + B_a/B_t\right]/2 \tag{10}$$

Hence, as long as B_a/B_t is known, $E(D)$ or $T_m(D)$ can be obtained. However, the shape and size of the nanoparticle must be known because both of them determine the B_a and B_t values. As is known, nanoparticles are a state of matter that has properties different from either molecules or bulk solids, and thus their shape and structure of nanoparticles are strongly functions of the number of atoms (N) in a system [32,33]. However, a nanoparticle with certain size usually has similar spherical shape in order to minimize surface energy although they could be in different structures [32], since surface energy directly determines the stability of different shapes and sizes, especially for the particles from ~1 nm to ~100 nm. Moreover, with size dropping, nanoparticles usually take the densest packing structure, for example, Na and Mo nanoparticles would have an FCC or more like icosahedron structures and Co nanoparticles with $4 \le N \le 60$ have an icosahedron structure [32], while the structure becomes unstable for a large number of atoms and transforms into a cubo-octahedron, which is just a patch of the fcc lattice [2]. Here, the ratio of surface to volume δ, where $\delta = N_s/N$, is used as mentioned in Jiang's work [32]. Since δ is the simplest function to describe the shape effect of nanoparticles, the smaller the δ value, the more spherical the shape, and thus the smaller surface energy. It is clear that the same δ value for both cuboctahedron and icosahedron is found [32] and this δ is the smallest value compared with other shapes. Thus, taking cuboctahedral shape to describe small nanoparticles becomes in valid within the acceptable error range. As size increases, $\delta \to 0$ for any shape, that is to say the shape effect will disappear for larger particles. In addition, it is commonly observed that most of fcc particles correspond to the cuboctahedral shape [33], and even can be extended to most closely packed materials, which is confirmed in Ref. [30] where the most appropriate structure of the nanoparticles can also be cubo-octahedron. Based on the discussion above, taking cuboctahedral structure as the shape of nanoparticles in this work is reasonable.

Next, the geometrical characteristic of cuboctahedral shape is introduced. In fact, cuboctahedral shape is a truncated octahedron of fcc crystals, where surface consists of 6 (100) facets and 8 (111) facets with distinct surface energy since the different coordination number on this two facets. However, we need not consider this difference in this work, because the parameter of bond number B_a or B_t has included the coordination number of all atoms at different site and thus considered the surface energy difference. Here we just assume that the cubo-octahedral structure has a central site, around which the nanoparticles grow (i.e., the number of concentric shells (n) around the central site defines the nanoparticle size). The zeroth order corresponds to the central site. The first-order nanoparticle is formed by adding a shell with a number of sites such that they cover the central site and form a surface with a cubo-octahedral shape. According to this method, the B_a/B_t of cubo-octahedral nanoparticles can be determined [30],

$$B_a/B_t = \frac{2n(5n^2+3n+1)}{10n^3+15n^2+11n+3} \tag{11}$$

In Eq. (11), the vacancies or defects in the nanoparticles cannot be easily calculated. The relation between the diameter D and number of shells n can be deduced as follows:

$$D = h(1+2n) \tag{12}$$

where h is the atomic distance.

Substituting Eq. (11) into Eq. (10) enables the determination of the $T_m(D)$ and $E(D)$ function of the nanoparticles:

$$\frac{T_m(D)}{T_{m0}} = \frac{E(D)}{E_0} = \left\{\left[\frac{2n(5n^2+3n+1)}{10n^3+15n^2+11n+3}\right]^{1/2} + \frac{2n(5n^2+3n+1)}{10n^3+15n^2+11n+3}\right\}\Big/2 \tag{13}$$

where $n = 1/2(D/h-1)$.

3. Results and discussions

Fig. 1 compares the predictions based on Eq. (13) with the experimental and molecular dynamic simulation results for the $T_m(D)$ values of the fcc elements, such as Al, Au, Pb, or Ar nanoparticles. As expected, $T_m(D)$ decreases with decreased D because of the reduced B_a value. Fig. 1 also shows the good agreement of the predictions with the experimental and molecular dynamic simulation results. This finding suggests the validity of the cubo-octahedron in describing the melting behavior of fcc nanoparticles. For comparison, the estimation of the $T_m(D)$ function of the icosahedral structure with $B_a/B_t = n(20n^2+15n+7)/20n^3+30n^2+22n+6$ [30] is also plotted as red lines in Fig. 2. The small difference between the icosahedron and cubo-octahedron models further confirms the success of the cubo-octahedron in predicting $T_m(D)$ values even for small nanoparticles with icosahedral structures. Eq. (13) is also used to estimate the $E(D)$ values for W and Mo nanoparticles, as shown in Fig. 3 for comparison with the corresponding experimental results. Considering that $D \to \infty$, then $E(D) \to E_0$ because $B_a/B_t \to 1$. Thus, the broken bond number can be neglected for larger D values. To some extent, the agreement between the model predictions and experimental results for W nanoparticles with $D \approx 1$ nm, suggests that small W particles may have closely packed structures, although their bulk structure is not closely packed. As expected from the experimental results, the simulation observations [34] for both W and Mo are also found to be consistent with the model predictions using Eq. (13), as shown in Fig. 3. In fact, Eq. (13) can also be used for clusters with small atomic numbers, such as Ni [35], Fe [36], and Au [37]. These results show the same depression in melting point as a function of the inverse of particle size. Eq. (13) is further proved to be reasonable based on the results shown in Fig. 4 for tetragonal elements, such as In and Sn, and even for the rhobohedral Bi element. (For interpretation of the references to color in this paragraph, the reader is referred to the web version of this article.)

Figs. 1–4 show the suitability of the cubo-octahedron, especially for larger particles with $D > 10$ nm. The reason is that the change in bond energy compared with that in the bulk interior is small, and that $B_a \to B_t$ for large particles. Notably, the melting point in Eq. (13) is considered to be proportional to the cohesive energy, which means that at the melting temperature, the total atomic bonding energy in the solid particles is equal to that in the liquid ones. Hence, all reported melting points in this work can be regarded as the phase-transformation temperature from solid to liquid, although the actual melting process is not considered. In fact, melting is a complicated process. As presented in Refs. [38,39], melting occurs from the surface to the interior for large particles only when $\Delta\gamma = \gamma_{sv} - \gamma_{sl} - \gamma_{lv} > 0$ (where γ_{sv}, γ_{sl}, and γ_{lv} are the solid–gas, solid–liquid, and liquid–gas interface energies, respectively), or through the entire volume for particles a few nanometers in size. As the temperature increases and gradually approaches the melting point, the thickness of the surface-melting layer increases depending on the pushing of the solid-melt interface into the interior. A critical value exists for the surface melting layer thickness, where the energy barrier for melting is the largest. The effect of this critical value on the melting point and even its intrinsic relationship with the particle size shall be clarified in our next work. This effect is similar to the demonstration in Ref. [38] that the ratios of the width of the solid–gas interface to the width of the solid-melt interface also play an important role on melting point.

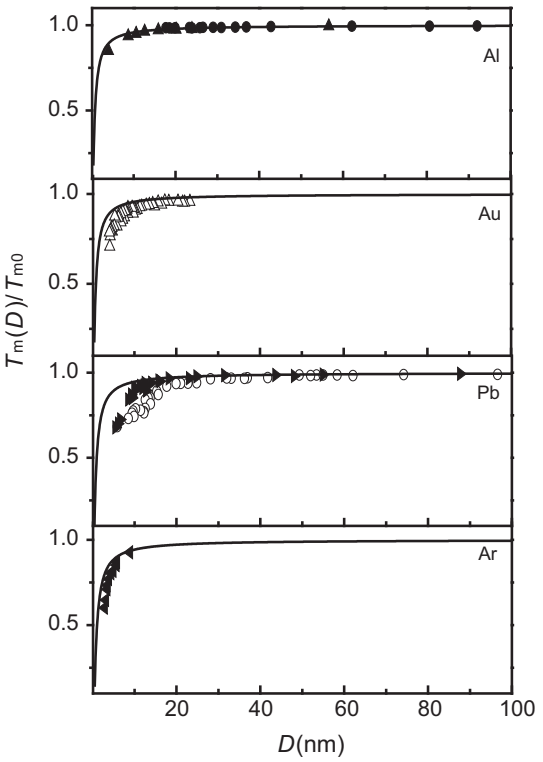

Fig. 1. $T_m(D)$ function for the nanoparticles of fcc elements in terms of Eq. (13) (black solid lines) where h = 0.3164 nm, 0.3188 nm, 0.3898 nm and 0.4249 nm [40], respectively for Al, Au, Pb and Ar. Symbols ▲ [41], ● [42], △ [6], ► [43], ○ [44] show the experimental results, and ◄ [45] the molecular dynamic simulation ones.

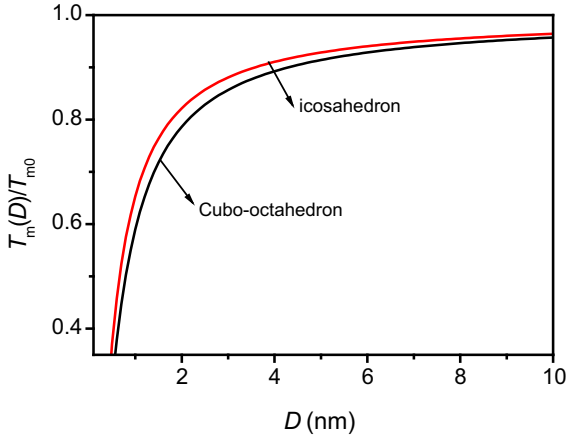

Fig. 2. The influence of Al particle shape on the size effect of melting temperature with the help of Eq. (13). For icosahedral and cubo-octahedral shape, the similar form to Eq. (10) is sure but the determination of bond number which can be found in Ref. [13].

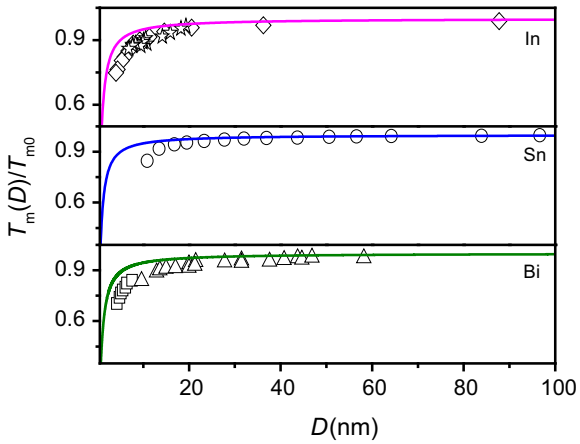

Fig. 4. Model predictions of $T_m(D)$ according to Eq. (13) for In, Sn, and Bi nanoparticles, where $h = 0.3682$ nm, 0.3724 nm and 0.4073 nm [40], respectively. The symbols ☆ [10], ◇ [47], ○ [48], △ [47], and □ [49] show the experimental results.

The assumption used in Eq. (10) is not always suitable for small particles, because only the surface bond relaxation is considered. In fact, except for surface atoms, interior atoms also become unstable compared with those of the bulk interior, resulting in an overestimation of Eq. (13). The defect or vacancy in a nanoparticle (i.e., the result of the ideal crystal using Eq. (13)) is also not considered in this work. This non-consideration may lead to a small overestimation of Eq. (13), which is necessary for small particles, as presented in Figs. 1–4. Despite the existing errors, Eq. (13) can still be regarded as a valid and simple way to predict $T_m(D)$ or $E(D)$ values even within the full size range. For small nanoparticles with $D < 5$ nm, the validity of Eq. (13) implies that the nanoparticles have closely packed structures regardless of the bulk of the structure. According to Eq. (13), the trend of the $T_m(D)$ or $E(D)$ values with size depends on the atomic distance when D is given. Thus, to determine the contribution of atomic distance, In, Sn, and Bi nanoparticles are compared and small differences are observed (Fig. 5). This result indicates that the atomic distance effect can be ignored for simplicity. From a thermodynamic perspective, the melting point is usually determined in terms of the surface energy, but the reverse is also true. Hence, the scale effect on the surface energy of nanoparticles can also be determined using Eq. (13).

To further confirm the validity of Eq. (13), the model predictions are compared with the theoretical results of Safaei and Shandiz [29] and Sun et al. [26] in Fig. 6. In fact, all of the models work well in simulating the size-dependent trends of melting points since similar consideration is taken, that is atomistic insight into this melting matter from the perspective of equilibration between the thermal energy of melting and the cohesive energy of an atom at different site and link all the melting behaviors involved to the effect of surface coordination number (CN) imperfection. Three models do not need to consider the latent energy of fusion, the mass density, and the surface/interface energy of different phases. Actually, the surface and interface energy and the local mass density of liquid and solid are functions of atomic separation and bond energy that are subject to the effect of CN imperfection [26]. However, the difference among three models predictions is inevitable as shown in Fig. 6. Although the same shape of cuboctahedron for nanoparticles is used, the ignorance of the bond energy increases as a result of surface CN imperfection, induces the underestimate of Safaei and Shandiz's model, while the extent of underestimation is more significant in Sun's model predictions compared with Eq. (13) in Fig. 6. In Sun's model, the effective coordination number usually takes the value of $z_1 = 4$ and $z_2 = 6$ respectively for the outermost two atomic layers; and at the lower end of size limit of a spherical dot, z_1 takes 3 or smaller. For Al nanoparticles, outermost three atomic layers are considered as

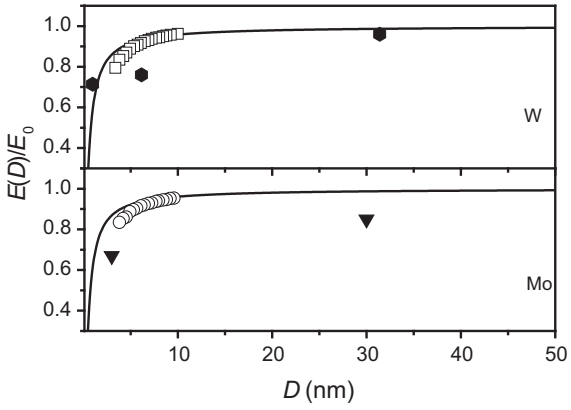

Fig. 3. The comparison of $E(D)$ values of model prediction for W and Mo nanoparticles based on Eq. (13) (solid lines) with $h = 0.3098$ nm and 0.290 nm [34], where experimental results ⬟ and ▼ [46], and simulation results □ and ○ [34] are clear.

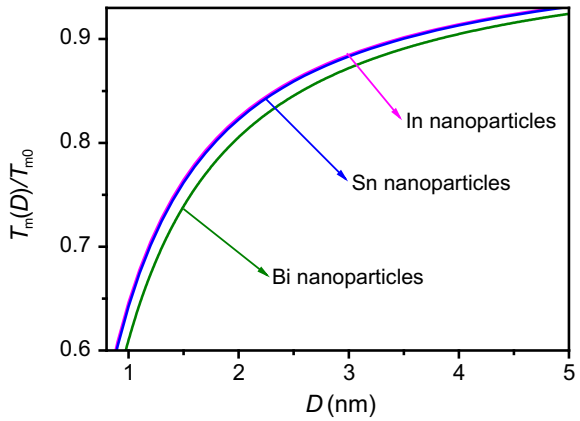

Fig. 5. The comparison of $T_m(D)$ values for In (red line), Sn (blue line) and Bi (green line) nanoparticles accounts for the effect induced by atomic distance. (For interpretation of the references to color in this figure legend, the reader is referred to the web version of this article.)

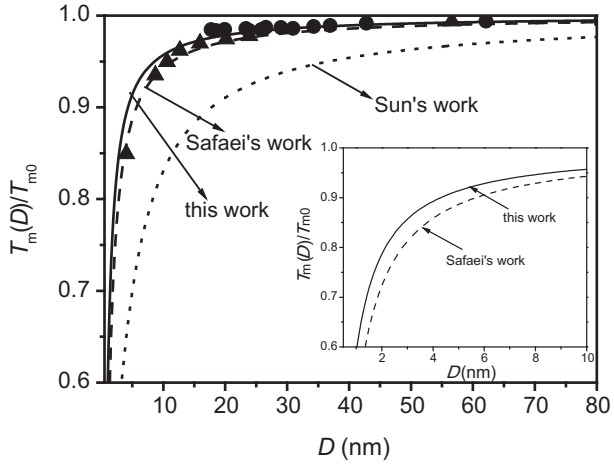

Fig. 6. The comparison of model predictions of Eq. (13) (solid line), the theoretical results from Shandiz and Safaei [29] (dashed line) and Sun et al. [26] (dotted line) for Al nanoparticles, with the experimental results denoted as the same symbols with that in Fig. 1 caption.

surface layers with CN imperfection, with $z_1 = 4$, $z_2 = 6$ and $z_3 = 8$ being used. So the bond imperfection in Sun's model is more grievous than our model. Except this, the most different thing is the shape factor, and spherical shape is taken in Sun's model [26]. That is why the better agreement with experimental results of Eq. (13) than that of Sun's model. However, we would like to indicate that all of the models are correct, relating the melting to the cohesive energy, though they are based on different premises. Compared with the existing models, the shape (or structure), bond imperfection of atoms at different site and the corresponding bond relaxation effect are considered in the current premise. Secondly, Eq. (13) involves almost no freely adjustable variables but the equilibrium atomic distance and particle size, that is $T_m(D)/T_{m0}$ follow the change of the portion of surface atoms of the solid. However, the melting point varies from site to site if the sample contains atoms with different CN [26]. Thus, shape is an important factor to determine melting point of nanoparticles especially for small size, while it has smaller influence on the values of $T_m(D)/T_{m0}$ since small errors induced from surface to volume ratio for different shape [32]. Thus, based on the consideration of cuboctahedral shape, Eq. (13) can be used for describing the extend of melting point decrease, within the acceptable error range, for many metallic nanoparticles and even metallic clusters even if their structures or shapes, surface energy, and even other thermodynamic information are unknown.

4. Conclusion

Based on bond number calculations, a united model independent of any adjustable parameter is developed for predicting the size-dependent melting point or the cohesive energy of nanoparticles. With decreased size, $T_m(D)$ or $E(D)$ decreases with decreased bond number. The agreement of the theoretical predictions with the experimental and simulation results for Al, Au, Pb, Ar, W, In, Sn, and Bi nanoparticles confirms the validity of the model.

Acknowledgements

The authors acknowledge the financial supports of the National Natural Science Foundation of China under (Grant No. 51101067), Natural Science Foundation of Anhui Higher Education Institutions of China (No. KJ2012B159) and Huaibei Normal University (No. 700435).

References

[1] G. Schmid, M. Baumle, M. Geerkens, I. Helm, C. Osemann, T. Sawitowski, Chem. Soc. Rev. 28 (1999) 179.
[2] J.M. Montejano-Carrizales, F. Aguilera-Granja, J.L. Moran-Lopez, Nanostruct. Mater. 8 (1997) 269.
[3] F. Baletto, R. Ferrando, Rev. Mod. Phys. 77 (2005) 371.
[4] Q. Jiang, Z. Zhang, J.C. Li, Chem. Phys. Lett. 322 (2000) 549.
[5] S. Xiong, W. Qi, Y. Cheng, B. Huang, M. Wang, Y. Li, Phys. Chem. Chem. Phys. 13 (2011) 10652.
[6] P. Buffat, J.P. Borel, Phys. Rev. A 13 (1976) 2287.
[7] V.P. Skripov, V.P. Koverda, V.N. Skokov, Phys. Status Solidi A 66 (1981) 109.
[8] G. Guisbiers, Nanoscale Res. Lett. 5 (2010) 1132.
[9] A. Safaei, J. Nanopart. Res. 12 (2010) 759.
[10] M. Zhang, M. Efremov, F. Schiettekatte, E.A. Olson, A.T. Kwan, S.L. Lai, T. Wisleder, J.E. Greene, L.H. Allen, Phys. Rev. B 62 (2000) 10548.
[11] K. Hoshino, S. Shimamura, Philos. Mag. A 40 (1979) 137.
[12] V.I. Ivlev, Sov. Phys. Solid State 33 (1991) 909.
[13] Z.H. Jin, P. Gumbsch, K. Lu, E. Ma, Phys. Rev. Lett. 87 (2001) 055703.
[14] B. Vekhter, R.S. Berry, J. Chem. Phys. 106 (1997) 6456.
[15] R. Defay, I. Prigogine, Surface Tension and Adsorption, Wiley, New York, 1951.
[16] K.F. Peters, J.B. Cohen, Y.-W. Chung, Phys. Rev. B 57 (1998) 13430.
[17] P.Z. Pawlow, Phys. Chem. 65 (1909) 1.
[18] H. Reiss, I.B. Wilson, J. Colloid Sci. 3 (1948) 551.
[19] H. Sakai, Surf. Sci. 351 (1996) 285.
[20] C.R.M. Wronski, J. Appl. Phys. 18 (1967) 1731.
[21] K.J. Hanszen, Z. Phys. 157 (1960) 523.
[22] H. Reiss, P. Mirabel, R.L. Whetten, J. Phys. Chem. 92 (1988) 7241.
[23] P.R. Couchman, W.A. Jesser, Nature (London) 269 (1977) 481.
[24] R.R. Vanfleet, J.M. Mochel, Surf. Sci. 341 (1995) 40.
[25] F.G. Shi, J. Mater. Res. 9 (1994) 1307;
C.Q. Sun, Prog. Mater. Sci. 54 (2009) 179.
[26] C.Q. Sun, Y. Wang, B.K. Tay, S. Li, H. Huang, Y.B. Zhang, J. Phys. Chem. B 106 (2002) 10705.
[27] Q. Jiang, H.M. Lu, M. Zhao, J. Phys. Condens. Matter 16 (2004) 521.
[28] F. Guinea, J.H. Rose, J.R. Smith, J. Ferrante, Appl. Phys. Lett. 44 (1984) 53.
[29] M.A. Shandiz, A. Safaei, S. Sanjabi, Z.H. Barber, Solid State Commun. 145 (2008) 432.
[30] M. Mirjalili, J. Vahdati-Khaki, J. Phys. Chem. Solids 69 (2008) 2116.
[31] D. Liu, J.S. Lian, Q. Jiang, J. Phys. Chem. C 113 (2009) 1168.
[32] H. Li, M. Zhao, Q. Jiang, J. Phys. Chem. C 113 (2009) 7594. and references therein.
[33] M.J. Yacamán, J.A. Acencio, H.B. Liu, J. Gardea-Torresdey, J. Vacuum Sci. Technol. B 19 (2001) 1091.
[34] Y. Shibuta, T. Suzuki, J. Chem. Phys. 129 (2008) 144102.
[35] Y. Qi, T. Çağin, W.L. Johnson, W.A. Goddard, J. Chem. Phys. 115 (2001) 385.
[36] F. Ding, A. Rosén, S. Curtarolo, K. Bolton, Appl. Phys. Lett. 88 (2006) 133110.
[37] Y.G. Chushak, L.S. Bartell, J. Phys. Chem. B 105 (2001) 11605.
[38] V.I. Levitas, K. Samani, Nat. Commun. 2 (2011) 284.
[39] V.I. Levitas, M. Javanbakht, Phys. Rev. Lett. 105 (2010) 165701.
[40] Table of Periodic Properties of the Elements, Sargent-Welch Scientific Company, Skokie, 1980.
[41] S.L. Lai, J.R.A. Carlsson, L.H. Allen, Appl. Phys. Lett. 72 (1998) 1098.
[42] J. Sun, S.L. Simon, Thermochim. Acta 463 (2007) 32.
[43] C.J. Coombes, J. Phys. F Metal. Phys. 2 (1972) 441.
[44] T.B. David, Y. Lereah, G. Deutscher, R. Kofman, P. Cheyssac, Phil. Mag. A 71 (1995) 1135.
[45] F. Cellestini, R.J.M. Pellenq, P. Bordarier, B. Rousseau, Z. Phys. D 37 (1996) 49.
[46] H.K. Kim, S.H. Huh, J.W. Park, J.W. Jeong, G.H. Lee, Chem. Phys. Lett. 354 (2002) 165.
[47] G.L. Allen, R.A. Bayles, W.W. Gile, W.A. Jesser, Thin Solid Films 144 (1986) 297.
[48] S.L. Lai, J.Y. Guo, V. Petrova, G. Ramanath, L.H. Allen, Phys. Rev. Lett. 77 (1996) 99.
[49] G. Kellermann, A.F. Craievich, Phys. Rev. B 65 (2002) 134204.